ISSN: 0975-8585

Research Journal of Pharmaceutical, Biological and Chemical Sciences

Growth, Characterization and theoretical studies on nonlinear optical single crystal of L-Alanine Oxalate.

K Deepa[1], P Sanjay[2], N Indumathi[2], S Senthil[2], and J Madhavan[1]*.

[1]Department of Physics, Loyola College, Chennai, India
[2]Department of Physics, Government Arts College for Men, Nandanam, Chennai, India

ABSTRACT

A nonlinear optical L-alanine oxalate (LAO) single crystal was synthesized and successfully grown by slow evaporation technique at room temperature. The Crystal structure of the as grown crystals was determined by single crystal X-ray diffraction analysis and is compared with the powder X-ray diffraction and theoretically stimulated one. The functional groups are identified by Fourier transform infrared spectral analysis and compared with simulated spectrum. The nonlinear optical efficiency of L-alanine oxalate (LAO) was determined from Kurtz Perry powder technique and the efficiency is almost equal to that of standard KDP crystals. Thermal analysis (TG-DTA) reveals the purity of the crystal and the sample is stable up to the melting point. HOMO–LUMO energies and first order molecular hyper polarizability of L-alanine oxalate (LAO) have been evaluated using density functional theory (DFT) employing B3LYP functional and 6-31G (d,p) basis set. Dielectric constant and dielectric loss of L-alanine oxalate (LAO) are measured in the frequency range from 50 Hz to 5 MHz at room temperatures.

Keywords: Single crystal XRD, FTIR, DFT, Dielectric studies, TG –DTA,

Corresponding author

ISSN: 0975-8585

INTRODUCTION

Non Linear Optical (NLO) materials play a vital role in the fields of optical data storage, image processing, electro-optical switching devices, optical information processing and telecommunication. Organic NLO materials have high non linearity and rapid response as compared to inorganic compounds but they have poor physiochemical and thermal stability [1]. L-Histidine is one of the optically active amino acid having an imiadazole side chain with pKa near neutrality [2]. It acts both as a proton donor and proton acceptor. It also acts as a nucleophilic agent [3]. The molecular NLO active crystals have been intensively studied to establish the observed structure-function correlation through the computational modeling of molecules as the origin of the nonlinear optical response in such systems are governed by the electronic polarizability of the electrons at the molecular level [4] as well as the geometrical arrangement of the NLO-chromophores present in the molecular system. The sensitive understanding of the structural and electronic response properties of NLO materials have been provided extensively both experimentally and theoretically using the quantum mechanical density functional theory (DFT) approach by vibrational spectroscopy. The molecular structural properties such as their atomistic level energy, vibrational frequencies, transition moment directions, magnitudes of the normal modes of vibrations etc. can be simulated with great accuracies by theoretical computational methods. Considerable effort has been devoted to understand the vibrational, optical, nonlinear response and electronic structure properties of the molecule- based NLO active organic crystals by the DFT based quantum chemical analysis [5].In this paper, we report on synthesis, growth, and characterization of L-alanine oxalate (LAO) single crystals. The detailed vibrational spectral studies are aided by DFT calculations to elucidate the assignment of the vibrational spectra and the highest occupied molecular orbital (HOMO), lower unoccupied molecular orbital (LUMO) and the first order hyperpolarizability of this compound is examined. FTIR, Thermal behavior, dielectric nature and SHG efficiency of the material are also studied.

EXPERIMENTAL PROCEDURES

Equimolar amount of L-alanine and oxalic acid were dissolved in double distilled water to prepare the aqueous solution of LAO. In deionized water, L-alanine and oxalic acid are allowed to react by the following chemical reaction

$$CH_3CHNH_3COOH + H_2C_2O_4 \rightarrow C_5H_9NO_6$$

The synthesized salt of LAO was obtained by evaporating the solvent. The synthesized salt was used to measure the solubility of LAO in water (Figure.1). The supersaturated solution was prepared in accordance with the solubility data. The solvent was allowed to evaporate and numerous tiny crystals were formed at the bottom of the container due to spontaneous nucleation. The transparent and defect free ones among them were chosen as the seeds for growing bulk crystals. Good optical quality crystals of dimension up to 19x3x6 mm^3 were harvested after a period of 20−30 days. The photographs of as grown crystals of LAO are shown in Figure.2.

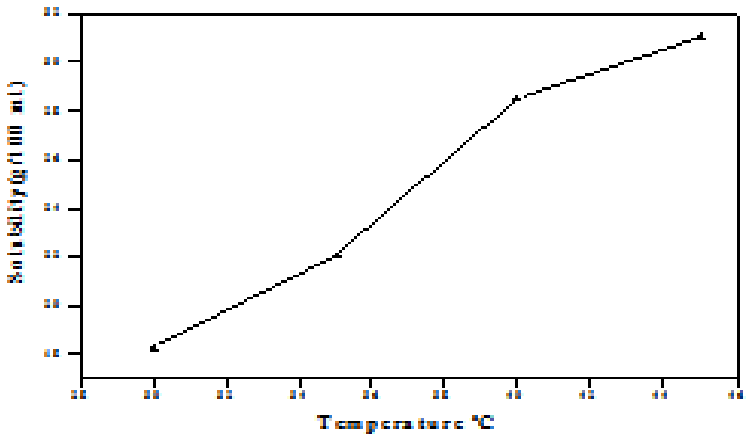

Figure 1: Solubility diagram of LAO

ISSN: 0975-8585

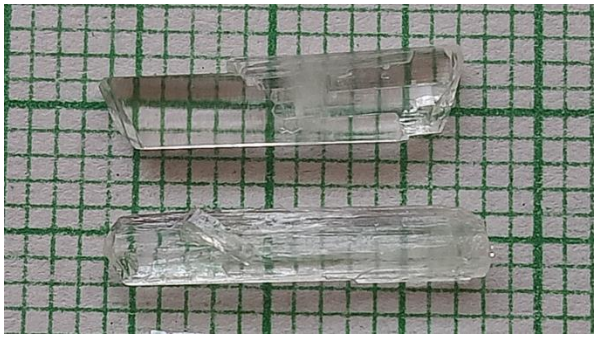

Figure 2: Photograph of as grown LAO single crystal

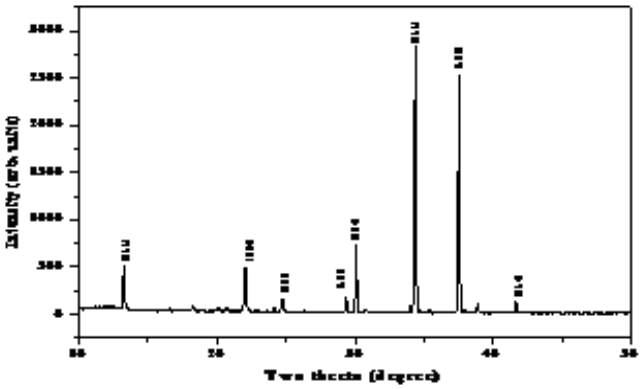

Figure 3: Experimentally obtained Powder XRD pattern of LAO

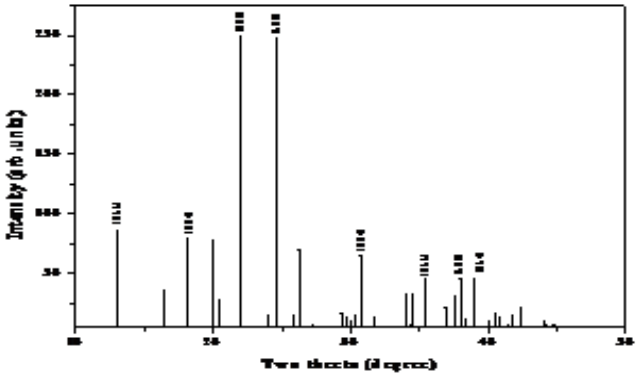

Figure 4: Theoretically simulated powder XRD pattern of LAO

Table 1: Crystal parameters of LAO

Empirical Formula	$C_5H_9NO_6$
Formula Weight	179.13
Temperature	293(2)K
Wavelength	1.54180A˚
Crystal System	Orthorhombic
Space Group	P $2_12_12_1$
Unit cell Dimensions	a = 5.6304(5) A˚ b = 7.2353(6)A˚ c = 19.597(3) A˚ $\alpha = \beta = \gamma = 90^{\circ}$

Volume	798.3(2) A°^{3}
Z	4
Calculated Density	1.490 g/cm^3
Absorption co- efficient	1.229mm^{-1}
F(0 0 0)	376
Crystal size	0.2 x 0.15 x 0.11 mm^3
Theta range of data Collection	4.51 – 67.91˚
Reflections collected	879
Independent reflections	853
Refinement method	Full matrix least squares on F^2
Data/restraints/parameters	853/0/112
Goodness – of – fit on F^2	1.092
Final R indices [I>2σ(I)]	R_1 = 0.0304 wR_2 = 0.0826
R indices (all data)	R_1 =0.0312 wR_2 = 0.0884

RESULTS AND DISCUSSION

SINGLE CRYSTAL XRD

The single crystal XRD was performed to analyze the structure of LAO crystal and the crystallographic parameters (Table 1). From single crystal XRD study of LAO crystal it was confirmed orthorhombic crystal system having non-centro symmetry with $P2_12_12_1$ space group. The lattice parameters are a=5.590(5) Å, b=7.198(6) Å, c=19.499(3) Å, α=β=γ=90˚ and the volume of the unit cells is found to be 798.3 (2) Å³. Theoretically simulated XRD pattern and experimentally obtained Powder XRD pattern are shown in Figure.3 and Figure.4 respectively. In the title compound, $C_3H_8NO_2^+$,$C_2HO_4^-$, the alanine molecule exists in the cationic form and the oxalic acid molecule in the mono-ionized state Independent part of unit cell contains eight monovalent L-Arg$^+$ cations, four $C_2HO_4^-$ anions and ten water molecules. L-arginine cations, oxalate-anions and water molecules are bonded with numerous hydrogen bonds. The alanine molecule exists in the cationic form with a protonated amino group and an uncharged carboxylic acid group. The oxalic acid molecule exists in a mono-ionized state. In the asymmetric unit, the L-alaninium cation and the semi oxalate anion are linked to each other through a N-H…O hydrogen bond. The head-to-tail hydrogen bond, with O_2 of the carboxyl group as acceptor, observed among the amino acid molecules in the crystal structure may be described as a zigzag sequence along the 2_1 screw axis along the direction of the a axis. The alaninium and semi-oxalate ions form alternate columns leading to a layered arrangement parallel to the ac plane and each such layer is interconnected to the other through N-H…O hydrogen bonds. Two short C-O contacts involving the carboxyl oxygen of the alaninium ion [C1…O2(y -1/2 + x, 3/ 2 -y,z) = 2.931 (3) A° and C2…O2(y -1/2 + x, 3/ 2 -y,z) = 2.977 (3) A°] are also observed in these layers. The slight difference observed in the bond lengths of C_5-O_5 and C_5-O_6 in the carboxylate group of the semi-oxalate ion may be attributed to the difference in the strengths of the N-H…O hydrogen bonds in which both O_5 and O_6 are involved.

COMPUTATIONAL DETAILS

A density functional theory investigation for minimum energy state of LAO molecule is carried out. In order to study the consequence of charge transfer LAO,its electronic property and the optimized structure were computed by using Gaussian 09 package and Gauss View [6]. Density functional theory (DFT) methods received much attention since one can simulate the electronic structure of the molecules. Structural optimization were carried in B3LYP/6-31þ G(d,p) level [7,8]. The optimized molecular structure was used to simulate the IR, Raman a hyper polarizability calculations. 1H and 13C NMR isotropic shielding were calculate dousing CDCl3 solvent effect by B3LYP/6- 31þG (d,p) method.

ISSN: 0975-8585

GEOMETRICAL STRUCTURE

The numbering system adopted for LAO in this investigation is shown in Figure.5. As there are two rotamers, viz., the Oxalic and the amino moieties, the molecule can exist in a variety of conformations. A B3LYP/6-31G(d,p) level on full geometry optimization with different spatial dispositions following the standard geometrical parameters, the converged final geometry was the one with all heavy atoms in a plane, with both the hydrogen atoms of the amino group and two of the hydrogen atoms of the methyl group lying out-of-plane. The relevant geometrical parameters like bond length and bond angles have been collected in Tables 2 and 3. It is found from the tables that minimum energy bond length and bond angles are compared with Single crystal XRD parameters. Bond lengths obtained from XRD analysis are smaller than Gaussian values. The differences between this can be attributed to the fact that the theoretical calculations were carried out with isolated molecules in the gaseous phase but the experimental values were based on molecules in the crystalline state [9].

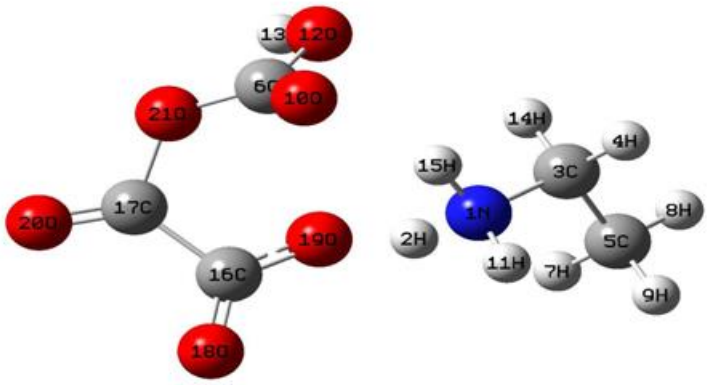

Figure 5: Atomic numbering systems adapted for ab initio computations of LAO molecule.

Table 2: Selected bond length of LAO molecule

S.No	Bondlength(A˚)	XRD	Gaussian
1	N_1- H_{15}	0.8900	1.03314
2.	N_1– H_{11}	0.8900	1.02123
3.	N_1– C_3	1.483(3)	1.50996
4.	C_3- H_{14}	0.9600	1.09283
5.	C_3– H_4	0.9600	1.09436
6.	C_3 – C_5	1.522(3)	1.52647
7.	C_5 – H_8	0.9600	1.09442
8.	C_5 – H_9	0.9800	1.09667
9.	C_5 – H_7	0.9800	1.09471
10	C_6 – O_{12}	1.199(2)	1.36148
11.	C_6 – O_{10}	1.219(2)	1.23060
12	C_6 – O_{21}	1.297(2)	1.38068
13.	O_{12} – H_{13}	0.8200	0.97978
14.	C_{17} – O_{21}	1.303(2)	1.46055
15.	C_{17} – O_{20}	1.205(2)	1.20749
16.	C_{17} – C_{16}	1.548(3)	1.54770
17.	C_{16} – O_{18}	1.235(2)	1.24278
18.	C_{16} – O_{19}	1.303(2)	1.30980

HYPERPOLARIZABILITY STUDIES

Interests in organic optoelectronic materials and devices have motivated experimental and theoretical studies of molecular structures with enhanced hyperpolarizabilities. [10]Molecules with electronic

asymmetry, or "push-pull" donor- bridge-acceptor electronic framework, have been demonstrated to have large first hyperpolarizabilities (β) [11] Interests in organic optoelectronic materials and devices have motivated experimental and theoretical studies of molecular structures with enhanced hyperpolarizabilities. Molecules with electronic asymmetry, or "push-pull" donor- bridge-acceptor electronic framework, have been demonstrated to have large first hyperpolarizabilities (β). The first static hyperpolarizability (β_0) and its related properties (β α_0 and Δα) have been calculated using B3LYP/6-31G level based on finite field approach. The components of β are defined as the coefficients in the Taylor series expansion of the energy in the external electric field.

To calculate the hyperpolarizability, the origin of the Cartesian coordinate system was chosen as the center of mass of the compound [12]. The calculated first hyperpolarizability of LAO is 2.84×10^{-30} esu which is 2 times that of KDP. The calculated first hyperpolarizability components are given in Table 4.

HOMO-LOMO ANALYSIS

HOMO and LUMO energies are the important parameters in quantum chemistry. By analyzing the molecular orbital energies one can get how the molecule interacts with other species in the crystal. The frozen orbital approximation and the ground state properties are used to calculate the excitation values. Both the highest occupied molecular orbital (HOMO) and the lowest unoccupied molecular orbital (LUMO) are the main orbital take part in chemical stability. The HOMO represents the ability to donate an electron, LUMO as an electron acceptor represents the ability to obtain an electron. The HOMO and LUMO energy calculated by B3LYP/6-31G(d,p) method are -0.25105a.u and -0.06410a.u respectively and HOMO–LUMO energy gap (B3LYP) = -0.18695a.u. The HOMO is located over the phenyl ring and the carboxylic acid group attached to the phenyl ring. The HOMO →LUMO transition implies an electron density transfer to the carboxylic acid group from the phenyl ring. Moreover, these orbital significantly overlap in their position for LAO Figure.6. The HOMO and LUMO energy gap explains the eventual charge transfer interactions taking place within the molecule. The HOMO-LUMO energy gap of the Molecule is found to be reduced due to the low value of the LUMO and the high value of the HOMO energies which are indicating an enhanced intermolecular charge transfer interactions in the system that leads the molecule as an easily polarizable one. The HOMO→LUMO charge- transfer transition for the molecule is obviously attributed to the π→π* type contributions. The extended π-conjugation and charge transfers signify a low energy gap which influences the nonlinear optical properties for LAO.

Table 3: Selected bond angles of LAO molecule.

Bond Angle(degree)	XRD	GAUSSIAN	Bond Angle(degree)	XRD	GAUSSIAN
H_{15}-N_1-H_{11}	109.5	110.79229	C_{17}-C_{16}-O_{19}	111.32	112.73023
H_{15}-N_1-C_3	109.5	111.47857	O_{20}-C_{17}-O_{21}	126.65(19)	117.81369
H_{11}-N_1-C_3	109.5	112.40390	C_{17}-O_{21}-C_6	120.5	121.77214
H_{14}-C_3-H_4	109.5	108.37728	O_{21}-C_6-O_{12}	109.5	111.57625
H_4-C_3-C_5	109.6	111.88045	O_{21}-C_6-O_{10}	125.65(18)	125.93896
H_7-C_5-H_8	109.5	108.24001	O_{12}-C_6-O_{10}	126.65	122.09844
O_{18}-C_{16}-O_{19}	126.7	129.51111	H_{13}-O_{12}-C_6	109.5	111.36942
C_{17}-C_{16}-O_{18}	118.05	117.75787	O_{10}-C_6-O_{12}	121.6	120.
C_3-C_5-H_8	109.5	109.5	H_{14}-C_3-C_5	109.65	111.46980

Table 4: Hyperpolarizability of LAO in esu

β_{xxx}	123.6388637
β_{xyy}	35.2443193
β_{xzz}	42.7272488
β_{yyy}	-3.1986838

ISSN: 0975-8585

β_{yzz}	3.6918875
β_{yxx}	-138.9561625
β_{zzz}	22.4016694
β_{zxx}	-5.5371442
β_{xyy}	38.7531654
$\beta_{tot(esu)}$	$2.09921105x10^{-30}$

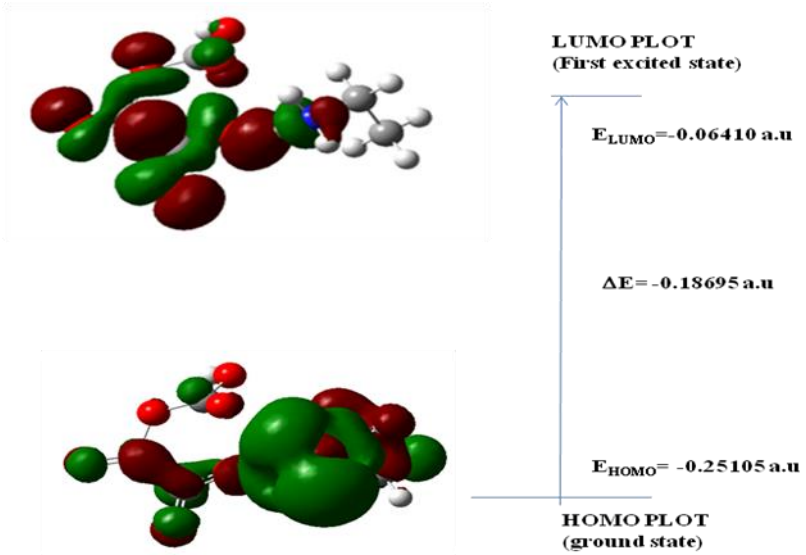

Figure 6: HOMO – LUMO plot of LAO molecule

Table 5: Vibrational Assignments of LAO Molecule

Frequency	Experimental frequency (cm^{-1})	Spectroscpic assignment	IR intensity (KM/Mole)	Force constant (mDyne/A°)	Reduced mass(amu)
3641.0169	-	NH st	71.9725	8.3194	1.0651
3525.2361	-	NH_2 asy st	49.3563	7.9127	1.0807
3331.6631	3341	OH st	177.1868	6.9319	1.0599
3158.8209	-	O-H st	14.8743	1.1057	1.1057
3146.7113	3135	C-H st	10.6923	6.4137	1.0994
3124.3879	-	CH_2 ips	10.0839	6.3190	1.0987
3090.9085	-	C-H st	13.8345	5.9790	1.0622
3054.0305	3030	NH_3asy st	13.5063	5.6998	1.0372
1828.7112	1814	C =O st	132.2124	23.9472	12.1539
1779.6634	-	C-C st	59.3880	4.3220	2.3161
1731.3753	1724	C =O st	403.0538	4.2672	2.4161
1727.1042	-	C=C st	255.0179	2.1343	1.2144
1688.1727	1692	C =N st	270.9033	2.1379	1.2732
1644.7270	1630	CH_2 ipb	865.4607	2.7875	1.7490
1557.4007	1560	NH_3 asy def	21.3002	1.5527	1.0865
1544.6808	1538	C=C st	15.2743	1.4739	1.0484
1537.6173	1513	NH_3 sy b	6.3549	1.4493	1.0404
1470.1417	1483	CH ipb	16.9270	1.5320	1.2031
1439.6680	1440	CH_2 sci	64.7713	1.6001	1.3103
1373.3448	1389	CH opb	13.5104	1.2841	1.1555
1293.6977	1309	CH_2 wag	877.1389	5.8857	5.9687
1287.6724	-	NH_3 tw	20.9560	1.4732	1.5080
1261.8902	-	OH ipb	45.4225	1.4083	1.5010

1255.8987	-	C-N st	158.1905	1.9490	2.0973
1191.6827	1146	CH_2 roc	29.4623	2.3333	2.7887
1076.3151	1102	OH ipb	29.5365	1.0936	1.6023
1060.6128	1069	PhI	24.6696	0.9601	1.4486
1020.8551	-	NH_2 t	15.5445	0.9602	1.5637
966.1956	991	R asyd	283.2435	6.2753	11.4091
962.8158	965	NH_3 roc	78.3274	7.2954	13.3571
880.0578	855	CC	3.6153	1.3124	2.8761
835.2978	819	CH opb	23.0544	0.4539	1.1042
794.7566	-	R opb	42.3301	4.3985	11.8190
784.3327	773	R berth	129.7208	4.1534	11.4592
686.8864	658	O-H opb	43.1214	3.4271	12.3284
670.7739	-	NH b	5.3482	2.7267	10.2858
600.6463	605	CN ipd	25.3086	1.9742	9.2878
586.6138	580	C-CO b	27.0439	2.1301	10.5061
548.2281	536	C-C b	135.7866	0.2126	1.2008
514.6009	522	COO^- roc	14.6141	0.2030	1.3011
468.8169	-	C-C b	107.1803	0.7797	6.0207
418.8364	-	C-C opb	20.5300	0.5787	5.5994
396.8678	-	R opb	3.1277	0.1898	2.0454
386.4879	-	C-C b	11.8996	0.6776	7.6994
355.1889	-	C-H	39.9763	0.4686	6.3036
294.3132	-	N-H st	17.3481	0.3921	7.6828
247.9294	-	NH_2 t	2.6787	0.0476	1.3145
204.8696	-	CO opb	5.7160	0.1551	6.2715
166.1278	-	C-C	21.7482	0.0793	4.8777
128.3344	-	C-C-N ipb	8.5613	0.0254	2.6186
100.6144	-	CC ipb	2.0537	0.0398	6.6733
89.6354	-	R tor	8.9999	0.0250	5.2862
63.3078	-	CNH_2 t	6.1209	0.0088	3.7280
47.9839	-	R tor	0.4398	0.0051	3.7536
39.9448	-	NH_3 tor	2.0039	0.0076	8.0795
31.7170	-	CC ben	0.0499	0.0026	4.3108

St-stretching ; **sym st**- symmetry stretching ;**asy st**- assymtry stretching ; **sci**-scisorring **t**-twisting ; **tor**-torsion ;**ipb**-in-planebending ; **opb**- out-of-plane bending; **ipd**-inplane deformation **wag**- wagging; **R**-anthracene ring;; **roc**-rocking;

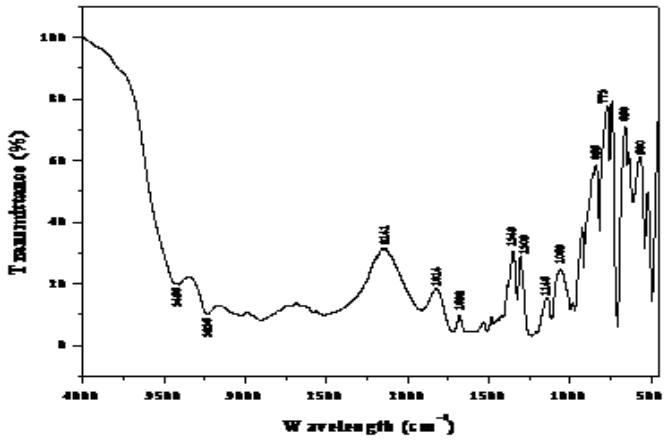

Figure 7: Experimentally obtained FTIR spectrum of LAO

ISSN: 0975-8585

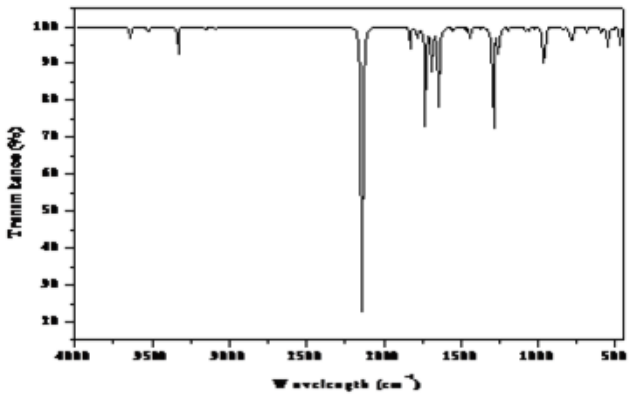

Figure 8: theoretically simulated FTIR spectrum of LAO

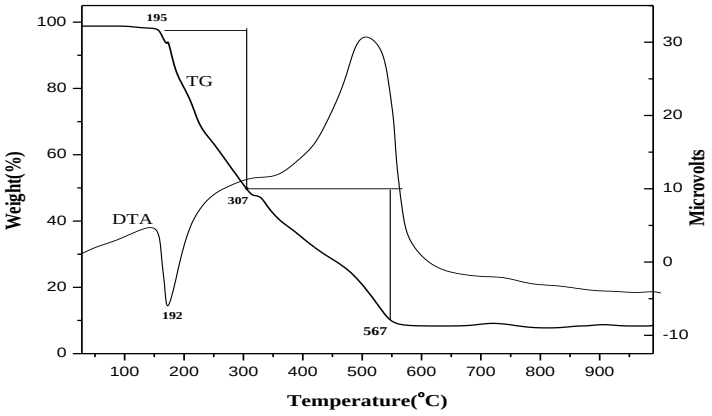

Figure 9: TG-DTA curves of LAO single crystals

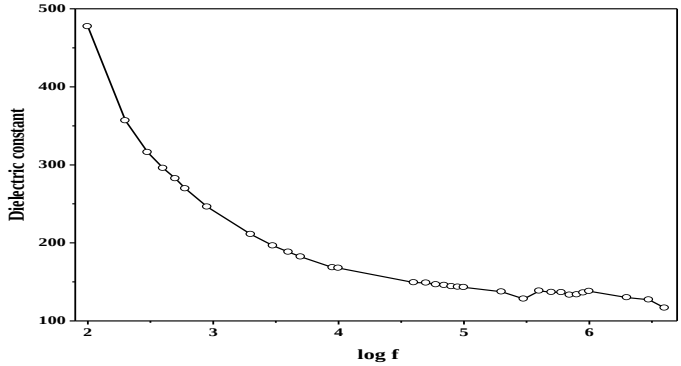

Figure 10: Variation of dielectric constant of LAO

ISSN: 0975-8585

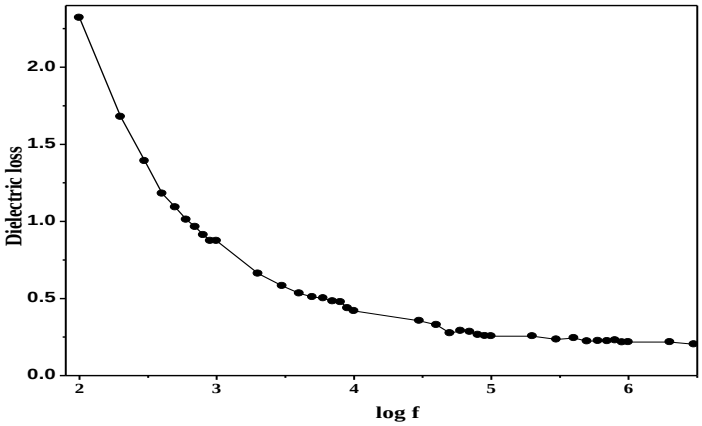

Figure 11: Variation of dielectric loss of LAO

VIBRATIONAL ANALYSIS

The LAO molecule has 21 atoms, which possess 57 normal modes of vibrations. All vibrations are active in infrared spectrum. The normal modes of LAM are distributed amongst the symmetry species as 39 in plane and 18 out plane vibrations. Usually the calculated harmonic vibrational wave numbers are higher than the experimental ones, because of the anharmonicity of the incomplete treatment of electron correlation and of the use of finite one-particle basis set. The harmonic frequencies were calculated by B3LYP method using 6-31G (d, p), basis sets experimentally observed and theoretically calculated harmonic vibrational frequencies and their correlations were gathered in Table 5. From the calculations, the computed values are in good agreement with the observed values. The FT-IR spectrum of LAO was recorded using BRUKER IFS-66V spectrometer in the range between 4000 and 500cm^{-1}. The resulting spectrum is shown in Figure.7. It coincides well with theoretically simulated FT-IR spectrum shown in Figure.8. Force constant, reduced mass and theoretically simulated IR intensity of the LAO molecule are given in Table 5.

NH_3 VIBRATIONS

The zwitterionic form molecules, the NH_3 asymmetric and symmetric stretching bands, normally appear in the region 3330 and 3080 cm^{-1}, respectively [13]. The strong band observed in IR vibrations at 3054 cm^{-1} corresponds to NH_3 asymmetric stretching mode. It has experimental counterpart at 3030 cm^{-1}. The red shifting of NH_3 stretching wave numbers indicate the formation of intramolecular N–H···O hydrogen Bonding. The short H . . . O distance (H13. . .O12 = 0.9797A˚) also supports the existence of N–H···O hydrogen bonding. The NH_3 asymmetric deformation vibrations usually appear in the region 1660–1610 cm^{-1} and that of the symmetric deformation in the region 1550–1485 cm^{-1} [14]. In LAO, the NH_3 asymmetric deformation vibrations are observed as a very strong band at 1557 cm^{-1} in IR and the symmetric bending modes are observed as a strong band in IR at 1537 cm^{-1}.Both the vibrations has its experimental values at1560 and1513 cm^{-1}. The NH_3 rocking modes appear as a weak band in IR at 962 cm^{-1} and torsions at 39 cm^{-1}.

CARBONYL VIBRATIONS

The C=O stretching vibrations give raise to the characteristic band in IR spectrum, and the intensity of these band can increase owing to the conjugation or formation of hydrogen bonds. The carbonyl stretching vibrations are expected in the region 1760–1730 cm^{-1} [15]. In LAO, there are three carbonyl groups (C6= O10, C16 =O18 and C17= O31). The very strong IR band at 1731 cm^{-1} correspond to C= O stretching modes and coincides with the experimental spectrum at 1724 cm^{-1}. When a carbonyl group participates in hydrogen bonding, resonance can occur, which puts a partial negative charge on the oxygen atom accepting the hydrogen bond and a positive charge on the atom donating the hydrogen, the partial 'transfer of allegiance' of the proton enhances resonance and lowers the C= O stretching wave number. The lowering of carbonyl stretching mode is attributed to the fact that the carbonyl group chelate with the other nucleophilic groups, thereby forming both intra and intermolecular hydrogen bonding in the crystal.

HYDROXYL VIBRATIONS

The OH stretching vibrations are sensitive to hydrogen bonding. The non-hydrogen-bonded or free hydroxyl group absorbs strongly in the 3600–3550 cm^{-1} region, whereas the existence of intermolecular hydrogen bond formation can lower O–H stretching wave number around 3500 cm^{-1} with increase in IR intensity [15]. This theory holds well in the present study. The strong bands observed in IR at 3331 and 3146 cm^{-1} correspond to OH stretching vibrations. The red shifting of OH stretching wave numbers are giving clear evidence for the intermolecular O–H· · ·O hydrogen bonding in the molecule. The in-plane bending of O–H group usually appears as strong bands in the region 1440–1260 cm^{-1} [14]. The strong bands at 1261 and 1076 cm^{-1} in the IR spectrum are assigned to OH in plane bending mode. The O–H out of plane bending vibration gives rise to a strong band in the region 700–600 cm^{-1} [15]. The calculated values of OH group vibrations are in good agreement with the experimental results.

NLO STUDIES

The SHG measuring set up consists of a Q switched Nd:YAG laser of 1064 nm whose beam falls on to a thin section of the material. The second harmonic green light at 532 nm is finally detected using an optical cable attached to a fluorescence spectroscope. For the SHG efficiency measurements, microcrystalline material of KDP was used for comparison. When a laser input of 6.2 mJ was passed through LAO, second harmonic signal of 122 mW is produced and the experimental data confirm a second harmonic efficiency of nearly 1 times that of KDP (124 mW).

THERMAL STUDIES

Thermal analysis provides information about the thermal stability of the as grown crystals. This is very important point when viewed in the perspective of fabrication techniques. The TG-DTA analyses were carried out in air at a heating rate of 20°C / minute for a temperature range of 30 – 1000°C and are represented in Figure 9. The material decomposes at 195°C. There is also no phase transition till the material melts and this enhances the temperature range for the utility of the crystal for NLO applications. The absence of water of crystallization in the molecular structure is indicated by the absence of the weight loss around 100°C. The endothermic peak in the the DTA curve at 192°C represents the melting point of the sample. The slope from 195°C to 307˚C in the TGA trace is due to the weight loss which may be attributed to liberation of gaseous fragments like carbon dioxide and ammonia. The decomposition of the main carbon chain starts at 307˚C due to the evolution of carbon dioxide. The decomposition of the resulting residue continues upto 1000˚C.The study of the material beyond this range is not of great significance for NLO studies.

DIELECTRIC STUDIES

The dielectric constant and the dielectric loss of LAO sample were measured using HIOKI 3532-50 LCR HITESTER in the frequency region 50 Hz to 5 MHz. Figure 10 shows the plot of dielectric constant (εr) versus log frequency. The dielectric constant has high values in the lower frequency region and then it decreases with the increase in frequency. The very high value of εr at low frequencies may be due to the presence of all the four polarizations, namely, space charge, orientational, electronic and ionic polarization and its low value at higher frequencies may be due to the loss of significance of these polarizations gradually. The variation of dielectric loss with frequency is shown in Figure 11 .The characteristics of low dielectric loss with high frequency for the sample suggest that it possesses enhanced optical quality with lesser defects and this parameter is of vital importance for nonlinear optical applications.

CONCLUSIONS

Good quality Single crystals of L-alanine Oxalate were grown by slow evaporation growth technique at room temperature. The single crystal analysis shows that the crystal belongs to orthorhombic crystal system with $P2_12_12_1$ space group. The powder X-ray diffraction study reveals the structure and crystallinity of the grown crystal land simulated pattern coincides with experimental one with varied intensity patterns. (DFT) computations of LAO molecule calculated by DFT (BLYP) level with 6-31G (d,p) basis set gives the optimized structure. Experimentally obtained bond lengths and bond angles are compared with theoretically calculated one. TG/DTA confirms that the crystal is stable up to 190°C and indicates it's thermally stability and suitability

in the field of laser application. The photoconductivity study ascertains the negative photoconductivity nature of the grown crystal. The dielectric constant and dielectric loss of L-alanine Oxalate single crystal also investigated as a function of frequency at room temperature. It indicates that the dielectric constant and dielectric loss of the materials decreases with increasing frequency. This property of the material can be used for the electronic applications. Theoretical and experimental IR spectroscopic analysis was carried out and the presence of functional groups in LAO molecule was qualitatively analyzed. HOMO-LUMO analysis reveals the molecular energy gap. The second harmonic generation of the grown crystal was measured and compared with KDP.

ACKNOWLEDGMENT

The authors acknowledge University Grants Commission (UGC), India, for funding this research project-F.No.4-4/2015-16 (MRP/UGC-SERO).

REFERENCES

[1] Gill AS. and Kalainathan S, Journal of Physics and Chemistry of Solids, 2011; 72: 1002-1007.
[2] Dmitriev V.G, Gurzadyan G.G, Nikogosyan D.N., Hand book of Nonlinear Optical Crystals, 2nd ed., Springer, New York, 1997.
[3] Senthil S, Pari S, Sagayaraj P, Madhavan J, Physica B: Condensed Matter,2009;404: 1655-1660.
[4] Hemalatha A, Deepa K, Venkatesan A, Senthil S, Mechanics, Materials Science & Engineering,2017:9: Doi 10.2412/mmse.85.63.511.
[5] Tanak H Y, Koysal S, Isik H, Yaman V, Ahsen Bull, Korean Chem. Soc, 2011;32(2): 673-680.
[6] Dennington R, Keith T, Millam J,GaussView 5,SemichemInc, Shawnee Mission, KS, 2009;
[7] Becke D, J. Chem. Phys, 1993;98(7): 5648–5652.
[8] Lee C, Yang W, Parr R.G, Phys.Rev, 1998;B3:7785–789.
[9] Madhavan J, Aruna S, Thomas P. C, Vimalan M, Rajasekar S. A, and Sagayaraj P, Cryst. Res. Technol, 2007; 1: 59-64.
[10] Miller D.A.B, and Chemla D.S, Physical Review B (Condensed Matter), 1987; 35:8113-8125.
[11] Victor Chow K, and Karen C, Denning, Journal of Econometrics, 1993; 58:385-401.
[12] Adant, M .Durpuis , JL Bredas, Int.J.Quantum Chem, 2004;56: 497-507.
[13] Chemla D. S. and Zyss J, "Nonlinear Optical Properties of Organic Molecule and Crystals," Academic press, New York, 1987.
[14] Silverstein R. M, Clayton Bassler G, and Morrill T. C, Spectroscopic Identification of Organic Compounds, 4th edition, John Wiley & Sons, New York, 1981.
[15] Colthup N.B, Daly L.H, Wiberley S.E, Introduction to Infrared and Raman Spectroscopy, Ed 3, Academic Press, New York, 1990; 301-305.